Journal of General Virology (2016), **97**, 1077–1086 DOI 10.1099/jgv.0.000441

Characterization of Nipah virus infection in a model of human airway epithelial cells cultured at an air–liquid interface

Olivier Escaffre,[1] Viktoriya Borisevich,[1] Leoncio A. Vergara,[2]† Julie W. Wen,[1] Dan Long[3] and Barry Rockx[1,4]

Correspondence
Barry Rockx
barry.rockx@rivm.nl

[1]Department of Pathology at University of Texas Medical Branch, Galveston, TX, USA

[2]Center for Biomedical Engineering at University of Texas Medical Branch, Galveston, TX, USA

[3]Rocky Mountain Veterinary Branch, Microscopy Unit, Division of Intramural Research, National Institute of Allergy and Infectious Diseases, National Institutes of Health, Hamilton, MT, USA

[4]Department of Rare and Emerging Viral Infections and Response (EID), Centre for Infectious Disease Control (CIb), National Institute of Public Health and the Environment (RIVM), Bilthoven, The Netherlands

Nipah virus (NiV) is an emerging paramyxovirus that can cause lethal respiratory illness in humans. No vaccine/therapeutic is currently licensed for humans. Human-to-human transmission was previously reported during outbreaks and NiV could be isolated from respiratory secretions, but the proportion of cases in Malaysia exhibiting respiratory symptoms was significantly lower than that in Bangladesh. Previously, we showed that primary human basal respiratory epithelial cells are susceptible to both NiV-Malaysia (M) and -Bangladesh (B) strains causing robust pro-inflammatory responses. However, the cells of the human respiratory epithelium that NiV targets are unknown and their role in NiV transmission and NiV-related lung pathogenesis is still poorly understood. Here, we characterized NiV infection of the human respiratory epithelium using a model of the human tracheal/bronchial (B-ALI) and small airway (S-ALI) epithelium cultured at an air–liquid interface. We show that NiV-M and NiV-B infect ciliated and secretory cells in B/S-ALI, and that infection of S-ALI, but not B-ALI, results in disruption of the epithelium integrity and host responses recruiting human immune cells. Interestingly, NiV-B replicated more efficiently in B-ALI than did NiV-M. These results suggest that the human tracheal/bronchial epithelium is favourable to NiV replication and shedding, while inducing a limited host response. Our data suggest that the small airways epithelium is prone to inflammation and lesions as well as constituting a point of virus entry into the pulmonary vasculature. The use of relevant models of the human respiratory tract, such as B/S-ALI, is critical for understanding NiV-related lung pathogenesis and identifying the underlying mechanisms allowing human-to-human transmission.

Received 13 November 2015
Revised 25 February 2016
Accepted 27 February 2016

INTRODUCTION

Nipah virus (NiV) is a zoonotic emerging pathogen of the family *Paramyxoviridae*, genus *Henipavirus* (Eaton *et al.*, 2005). NiV can cause severe acute and often lethal respiratory illness and/or encephalitis in humans and animals, and there are no approved vaccines or therapeutics for human use. In 1998–1999, a total of 276 human cases were reported during an outbreak of NiV infection in Malaysia and Singapore with a 38 % case fatality rate (CFR) (Chua *et al.*, 2000; Goh *et al.*, 2000). Since 2001, NiV outbreaks have occurred almost yearly in Bangladesh and India where the CFR can reach up to 100 % (Harit *et al.*, 2006; Hossain *et al.*, 2008). NiV infection has caused severe pneumonia or an acute respiratory-distress-like syndrome during the outbreaks in Malaysia (Chong *et al.*, 2002; Goh *et al.*, 2000; Paton *et al.*, 1999) and Bangladesh (Hossain *et al.*, 2008), respectively. Interestingly, the proportion of human cases in Malaysia exhibiting respiratory symptoms was less than 30 % as opposed to more than 70 % in Bangladesh (Lo & Rota, 2008). Respiratory distress was significantly associated with death in Bangladesh (Hossain *et al.*, 2008), and was not documented in Malaysia. In addition, human-to-human transmission was only reported during the outbreaks in Bangladesh

†Present address: Center for Translational Cancer Research (CTCR), Institute of Biosciences and Technology (IBT), Texas A&M Health Science Center, Houston, TX, USA.

(Gurley *et al.*, 2007). These data suggest that differences in virulence and transmission may exist between the genetically distinct NiV strains from Malaysia (NiV-M) and from Bangladesh (NiV-B). Histopathological changes in the lungs of NiV-M-infected cases were characterized by lesions and inflammation in the small airways (Valbuena *et al.*, 2014; Wong *et al.*, 2002), and both NiV-M and NiV-B were isolated from human respiratory secretions (Chua *et al.*, 2001; Hossain *et al.*, 2008; Mounts *et al.*, 2001; Tan & Tan, 2001). However, NiV pathogenesis in the human respiratory tract and specifically the role of the respiratory epithelium in NiV transmission and in the inflammation of the lung is largely unknown.

We hypothesize that the respiratory disease and transmission in humans is initiated by NiV infection of epithelial cells from the lower respiratory tract. Here, we characterized NiV-M and NiV-B infection of the human respiratory tract using differentiated epithelial models of the trachea/bronchi (B-ALI) and small airways (S-ALI) that closely mimic the anatomy of the human lower respiratory tract epithelium proximal to the alveoli. Our results show that ciliated and non-ciliated cells are permissive to both NiV-M and NiV-B infection, and that infection induces host responses that recruit human immune cells. Interestingly, NiV-B replicated more efficiently in the tracheal/bronchial epithelial model compared with NiV-M.

RESULTS

B- and S-ALI mimic the human lower respiratory epithelium

In order to determine whether these cultures resembled the human tracheal/bronchial and small airway epithelium, the phenotype of cells present in the B- and S-ALI cultures was characterized. B- and S-ALI cultures consisted of pseudostratified columnar and simple cuboidal respiratory-like epithelium, respectively (Fig. 1a, b). Both models contained ciliated cells (Figs 1c, d and 2a, d) but only B-ALI contained both Clara secretory cells and mucus-producing goblet cells (Fig. 2b, c). Goblet cells were not found in S-ALI (Fig. 2f). Altogether, this suggests that B- and S-ALI cultures resemble the human lower respiratory epithelium proximal to the alveoli.

NiV-M and NiV-B replicate in B- and S-ALI

To investigate NiV-M and NiV-B virus replication in the human tracheal/bronchial and small airway epithelium, B- and S-ALI cultures were infected at a high and low m.o.i. of 1 and 0.1, respectively. Regardless of the m.o.i. used, no cytopathic effect was observed from the apical side of B-ALI cultures due to infection while both NiV-M- and NiV-B-infected S-ALI cultures showed evidence of cell detachment from the insert starting at day 4 post-infection (p.i.) (data not shown). At a high m.o.i. in B-ALI, NiV-B replicated to significantly higher titres than did NiV-M at days 2 and 5 p.i. ($P<0.05$) (Fig. 3a). NiV-B and NiV-M virus titres peaked respectively at days 5 and 8 p.i., and peak titres were comparable. At a low m.o.i. in B-ALI, NiV-B also replicated to significantly higher titres by day 7 p.i. compared with NiV-M ($P<0.05$) (Fig. 3b). Interestingly, NiV-M virus titre remained under the limit of detection until day 10 p.i. In S-ALI, infection with a high m.o.i. resulted in higher replication of NiV-B compared with NiV-M starting at day 3 p.i., with significant differences at days 3–4 and 7–8 p.i. ($P<0.05$) (Fig. 3c). Both NiV-B and NiV-M virus titres reached a maximum as early as day 3–4 p.i. but peak titres were about 1 log higher for NiV-B compared with NiV-M. At a low m.o.i. in S-ALI, NiV-B also replicated with a higher titre compared with NiV-M, with significant differences at day 6–7 p.i. ($P<0.05$) (Fig. 3d). These results suggest that there are intrinsic differences between the NiV-M and NiV-B strains in their ability to replicate in the human tracheal/bronchial and small airway epithelium, with the NiV-B strain consistently replicating more efficiently, and that both NiV strains can disrupt the small airway epithelium integrity.

NiV-M and NiV-B have similar cell tropism in B-ALI

To determine which cell types were susceptible to NiV-M and NiV-B, immunofluorescence staining of viral antigen and markers for either ciliated, goblet or Clara cells was performed in B-ALI. Both NiV-M and NiV-B infected all three cell types as observed in B-ALI (Fig. 4a–f). Altogether, these results suggest that NiV-M and NiV-B have the same tropism for differentiated epithelial cells from the human lower respiratory tract proximal to the alveoli.

NiV-M and NiV-B induce a similar innate immune response in B- and S-ALI

To gain more insight into the immune response resulting from NiV-M and NiV-B infection of the human tracheal/bronchial and small airway epithelium, the levels of a panel of chemokines/cytokines were quantified in the basolateral media from B- and S-ALI cultures infected at a high m.o.i. and sampled on day 6 or 7 p.i. (Fig. 5). Among 16 different mediators tested, only the secretion levels of fractalkine, granulocyte-colony stimulating factor (G-CSF), granulocyte macrophage-colony stimulating factor (GM-CSF), IL-6, monocyte chemotactic protein (MCP-1) and chemokine ligand 10 (CXCL10) were significantly increased by NiV-M and NiV-B infection in the B- and/or S-ALI model. IFN-beta secretion levels in B- and S-ALI remained undetectable (data not shown). Overall, the baseline cytokine levels were higher in non-infected S-ALI compared with B-ALI. Despite the slight difference of virus replication between NiV strains in both B- and S-ALI, NiV-M and NiV-B induced a similar secretion level of chemokines/cytokines in B-ALI but at a much higher level in S-ALI, with the exception of GM-CSF. The largest increases in cytokine/chemokine secretion

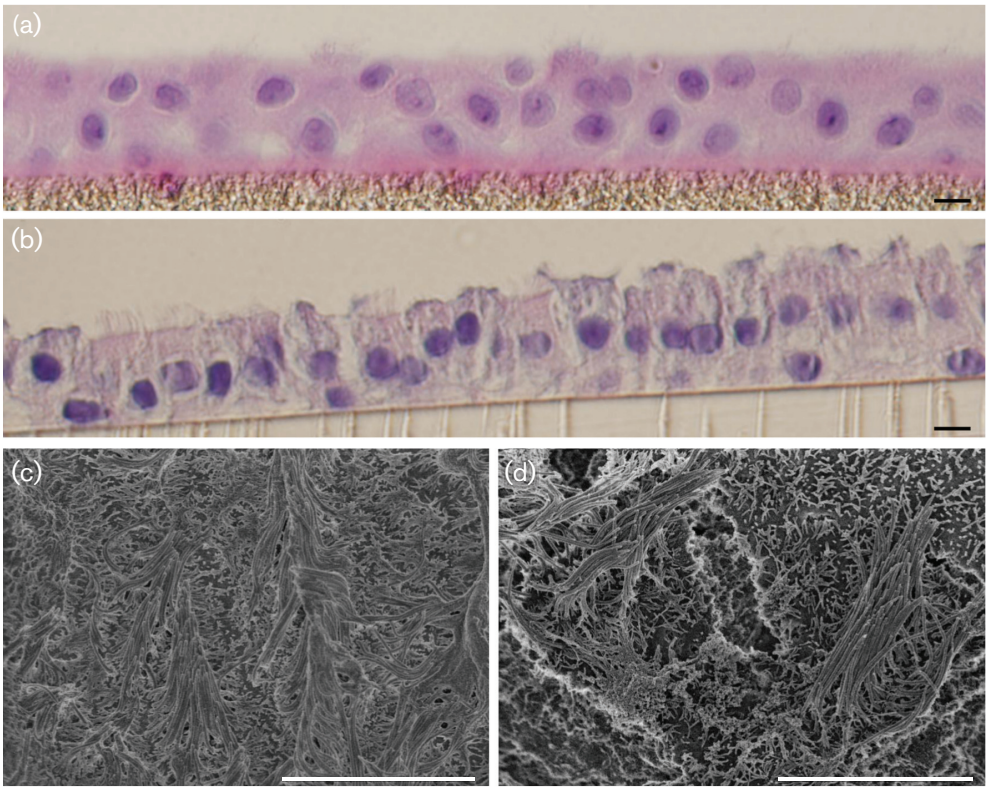

Fig. 1. Imaging of B- and S-ALI epithelium. Cross-section of B-ALI (a) and S-ALI (b) resembling a pseudostratified columnar and simple cuboidal respiratory-like epithelium, respectively. Magnification ×40. Bar, 10 μm. Scanning electron microscopy of B-ALI (c) and S-ALI (d) displaying cilia from ciliated cells. Magnification ×10 000. Bar, 10 μm.

levels due to NiV infection were observed for fractalkine, G-CSF and IL-6 in S-ALI ($P<0.001$), MCP-1 in B-ALI ($P<0.001$) and CXCL-10 in both B- and S-ALI ($P<0.001$) when compared with controls. These results suggest that NiV-M and NiV-B induce a comparable pro-inflammatory response in the tracheal/bronchial epithelium that is distinct from that in the small airway epithelium proximal to the alveoli.

NiV infection of S-ALI, but not of B-ALI, results in the recruitment of monocytes

To determine whether NiV-infection-mediated inflammatory response of the tracheal/bronchial and small airway epithelium can potentially recruit immune cells, cytokines/chemokines secreted in B- and S-ALI were tested for monocyte chemotactic activity. Since the media used for differentiated airway cultures interfered with chemotaxis, recombinant human cytokines/chemokines, at concentrations similar to those in the basolateral media of NiV-infected B- and S-ALI cultures, were assessed for monocyte chemotactic activity. No increase of monocyte migration was observed in the mixtures similar to the basal side of NiV-M- or NiV-B-infected B-ALI compared with that in control B-ALI (Fig. 6a). However, an equivalent increase of migrated monocytes occurred in the mixtures derived from the basal side of NiV-M- and NiV-B-infected S-ALI, when compared with that in control S-ALI ($P<0.05$) (Fig. 6a). Since the immune response of S-ALI to NiV-M and NiV-B infection was comparable, only the cytokine/chemokine concentration levels detected from NiV-M-infected S-ALI were subsequently tested individually, via the use of only one cytokine or chemokine at a time, against those of control S-ALI for monocyte chemotactic activity. The increased concentrations of fractalkine and IL-6 were enough to recruit more monocytes ($P<0.01$) (Fig. 6b), while those of G-CSF and CXCL-10 failed to do so (data not shown). These results suggest that, unlike the tracheal/bronchial respiratory epithelium, the small airway epithelium proximal to the alveoli can recruit monocytes via fractalkine and IL-6 secretion in response to NiV-M and NiV-B infection.

DISCUSSION

NiV is a zoonotic emerging virus that can cause severe and often fatal respiratory disease and/or encephalitis in humans (Rockx *et al.*, 2012). We have previously shown that the respiratory epithelium is an important target during the early stages of NiV infection (Escaffre *et al.*, 2013; Rockx *et al.*, 2011; Valbuena *et al.*, 2014); however, the molecular mechanisms of NiV-mediated pathogenesis

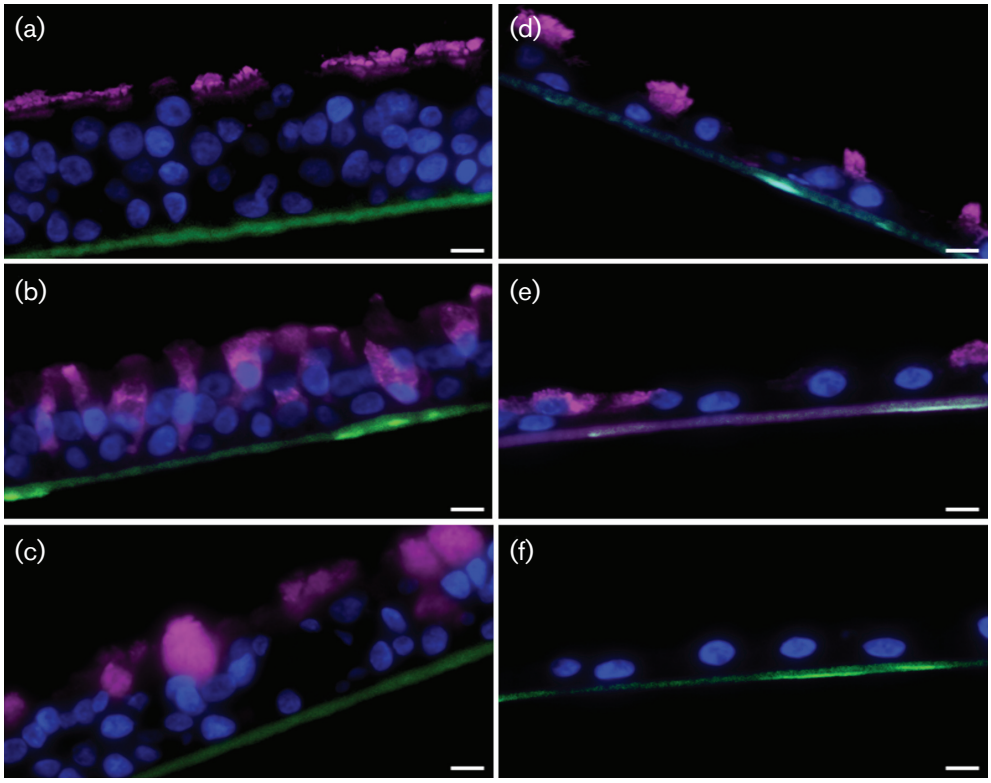

Fig. 2. Imaging of the most abundant populations of differentiated cells in B- and S-ALI epithelium. In magenta, cross sections showing cilia from ciliated cells in B-ALI (a) and S-ALI (d), CC10 protein from Clara cells in B-ALI (b) and S-ALI (e), and Mucin5AC from goblet cells in B-ALI (c). No staining of Mucin5AC in S-ALI (f). Cell nuclei in blue. Magnification ×40. Bars, 10 μm.

remain poorly understood. Here, a new model of NiV infection of the human tracheal/bronchial and small airway epithelium cultured at an air–liquid interface was used to investigate NiV-M and NiV-B cell tropism, virus replication and virus-induced immune response in epithelium of the lower respiratory tract proximal to the alveoli.

The human tracheal/bronchial epithelium consists of about 30 % ciliated cells, about 30 % secretory cells that are predominantly goblet cells with a few Clara cells, about 30 % of undifferentiated basal cells, less than 5 % of indeterminate cells together with a low percentage of neuroendocrine and brush cells (Levitzky, 2013; Mercer *et al.*, 1994; Rock *et al.*, 2010). The small airway epithelium proximal to the alveoli is populated at more than 50 % by ciliated cells and by a large proportion of secretory cells that are mostly Clara cells, but goblet and undifferentiated basal cells are no longer present. Indeterminate cells and a low population of neuroendocrine and brush cells may also be found (Levitzky, 2013; Mercer *et al.*, 1994; Rock *et al.*, 2010). Previous studies using the same B-ALI model reported the presence of ciliated cells and secretory goblet cells (Mitchell *et al.*, 2011; Ren *et al.*, 2012) but their respective proportions and the presence of other cell types in this model were, to our knowledge, not further investigated. Apart from the ciliated cells, the cellular composition of this particular S-ALI model has not been fully characterized either.

In this study, B- and S-ALI cultures resembled the human tracheal/bronchial and small airway epithelium due to their respective pseudostratified columnar and simple cuboidal respiratory-like epithelium arrangement, and also the distribution of ciliated, goblet and Clara cells (Levitzky, 2013). Several human respiratory epithelial cell models that resemble B-ALI have previously been used and are well-accepted for studying respiratory infections (Gerlach *et al.*, 2013; Lam *et al.*, 2015; Matrosovich *et al.*, 2004; Rockx *et al.*, 2007) as they are polarized and can be exposed to viruses in an *in vivo*-like manner, as opposed to culture-medium-submerged undifferentiated monolayer cells. Altogether, our data suggest that B- and S-ALI closely mimic the human lower respiratory tract epithelium proximal to the alveoli and therefore are biologically relevant models for studying NiV pathogenesis. Unfortunately, the matrix-coated microporous membrane of the inserts did not allow passage of virus particles towards the basal side, therefore impairing the study of virus penetration and dissemination via the epithelium.

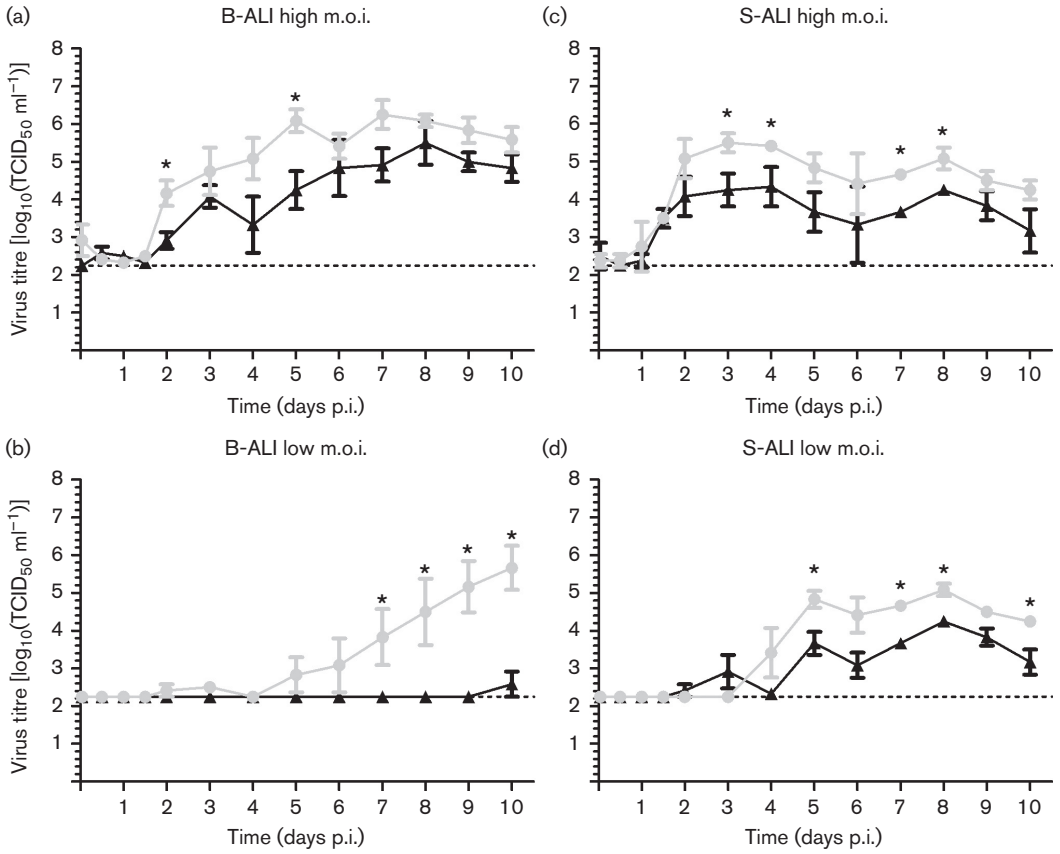

Fig. 3. NiV replication in B- and S-ALI at a high and low infective dose. Kinetic of NiV-M (in black) and NiV-B (in grey) replication in B-ALI (a, b) and S-ALI (c, d) for 10 days p.i. Results are expressed as the mean of three repetitions with the standard deviation. The horizontal dotted line corresponds to the detection limit. *$P<0.05$, non-parametric Mann–Whitney test.

Both NiV-B and NiV-M strains were isolated from human respiratory secretions (Chua *et al.*, 2001; Hossain *et al.*, 2008; Mounts *et al.*, 2001; Tan & Tan, 2001) and from the upper and lower respiratory tract epithelium in hamsters (Baseler *et al.*, 2015; de Wit *et al.*, 2014; Rockx *et al.*, 2011). In our B-ALI model, ciliated, goblet and Clara cells were susceptible to NiV-M and NiV-B. These same ciliated and Clara cells were also likely infected in S-ALI but could not be identified as the infection caused severe cellular damage. Both strains replicated efficiently in S-ALI whereas NiV-B replicated significantly faster and to a higher titre than NiV-M in B-ALI, suggesting intrinsic differences between NiV strains that result in more efficient NiV-B replication in the tracheal/bronchial epithelium, but not the small airways. Such difference of virus replication level could play a role in the differences observed in human-to-human transmission during outbreaks (Gurley *et al.*, 2007). In order to better study the possible intrinsic differences between the different NiV strains, an in depth comparison will be required using cultures from multiple donors.

We previously showed that NiV-M and NiV-B induced secretion of G-CSF, GM-CSF, IL-1α, IL-6 and IL-8, as well as CXCL10, MCP-1 and eotaxin, in supernatants of basal epithelial cells of the trachea/bronchia (NHBE) and the small airway (SAEC) (Escaffre *et al.*, 2013). In the present study, a reduced number of these inflammatory mediators, including G-CSF, GM-CSF, IL-6, MCP-1, fractalkine and CXCL10, also had increased concentration levels in NiV-M- and NiV-B-infected B- and S-ALI cultures, and were interestingly at much higher levels in the latter. Therefore, these results suggest that the immune responses of B- and S-ALI to both NiV strains are more restricted than those of NHBE and SAEC (Escaffre *et al.*, 2013), likely due to the differentiation of cells. In agreement with our previous observation in NiV-M- and NiV-B-infected NHBE or SAEC, there were no significant differences in cytokine and chemokine induction between NiV-M- and NiV-B-infected B- or S-ALI cultures (Escaffre *et al.*, 2013). These data suggest that both NiV strains induce a similar inflammation of the lower respiratory tract epithelium distal to the alveoli. However, it is likely that the strongest inflammation occurs in the small airway epithelium due to much higher levels of IL-6, CXCL10, G-CSF and fractalkine than in the tracheal/bronchial epithelium. This is supported by the fact that

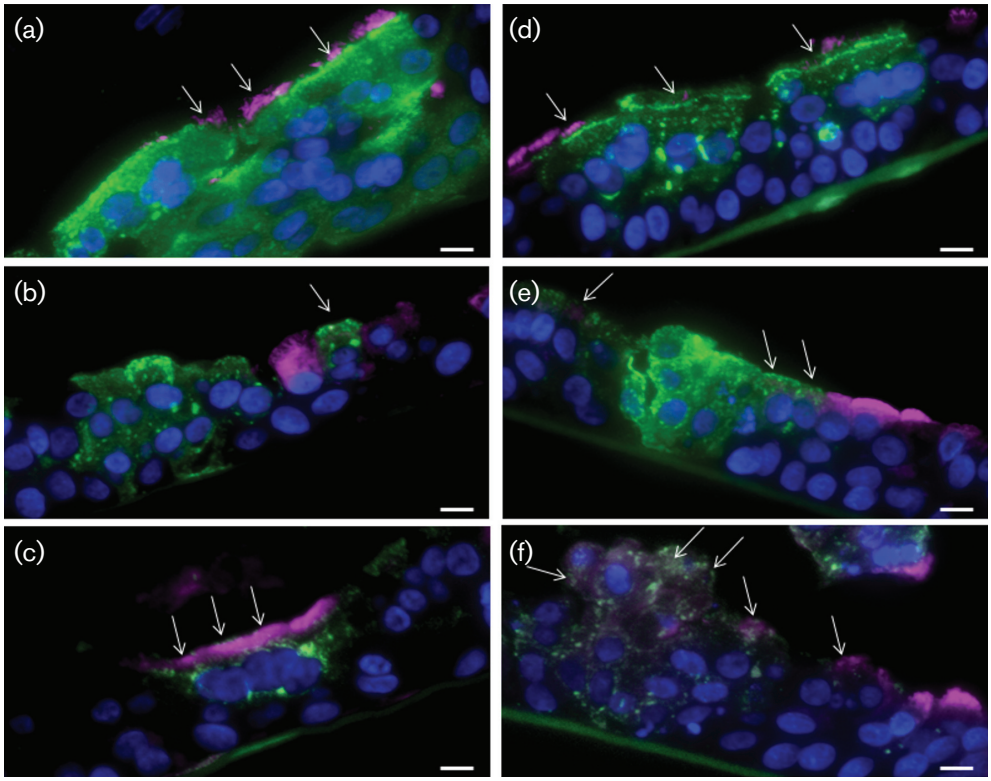

Fig. 4. NiV tropism for differentiated cells in B-ALI. B-ALI cross-sections showing NiV-M- and NiV-B-infected epithelial cells at day 4 p.i. Magnification ×40. NiV-M-infected (a) ciliated cells (virus in green, cilia in magenta), (b) Clara cells (virus in green, CC10 protein in magenta) and (c) goblet cells (virus in green, Mucin5AC protein in magenta). NiV-B-infected (d) ciliated cells (virus in green, cilia in magenta), (e) Clara cells (virus in green, CC10 protein in magenta) and (f) goblet cells (virus in green, Mucin5AC protein in magenta). Cell nuclei in blue. White arrows show NiV-infected ciliated, Clara or goblet cells. Bars, 10 μm.

increased secretion levels of these mediators were previously reported in NiV-M-infected lung grafts exhibiting syncytia formation in and around primitive alveolar spaces (Valbuena *et al.*, 2014). In addition, inflammation was only found in the small airways in NiV-M-infected human cases (Wong *et al.*, 2002). In hamsters, both NiV strains caused comparable lesions of the small airways (Baseler *et al.*, 2015), and IL-6 and CXCL10 gene upregulation in lungs also correlated with inflammation and pathogenesis (Rockx *et al.*, 2011).

Histopathological analyses of the lungs from several human cases of NiV-M infection showed fibrinoid alveolar necrosis but did not report the presence of inflammatory cellular infiltrates into the respiratory epithelium (Wong *et al.*, 2002). However, these data are only available from the late stage of disease, while infection of the respiratory epithelium occurs during the early stages of infection. Cytokines and chemokines, including those released from infected B- and S-ALI cultures, can act as migration factors of immune cells (Baggiolini *et al.*, 1992; Clahsen & Schaper, 2008; Eaton *et al.*, 2005; Imai *et al.*, 1997; Luster & Leder, 1993; Taub *et al.*, 1993; Thelen, 2001; Weissenbach *et al.*, 2004). We showed that monocyte chemotaxis occurred by cytokines and chemokines induced during NiV-M- and NiV-B-infection in S-ALI, but not in B-ALI samples, and was due to high concentrations of both IL-6 and fractalkine, two mediators known to have such role (Clahsen & Schaper, 2008; Imai *et al.*, 1997). Therefore, this suggests that the small airway respiratory epithelium proximal to alveoli is itself prone to recruit immune cells such as monocytes that will eventually differentiate into macrophages due to inflammation. These data are in line with a previous study showing macrophage infiltrations in the lumen of the small airway, but not in the bronchial epithelium, of NiV-M-infected pigs (Hooper *et al.*, 2001). Macrophages were also found in the terminal bronchioles and alveolar spaces of NiV-M- and NiV-B-infected hamsters (DeBuysscher *et al.*, 2013) and in alveolar spaces of NiV-M-infected African green monkeys (Bossart *et al.*, 2012). Interestingly, no IFN-beta was detected in our respiratory epithelium models as opposed to lung microvasculature endothelial cells where increased secretion levels caused by NiV-M correlated with enhanced monocyte and T-lymphocyte chemotaxis (Lo *et al.*, 2010), suggesting that IFN-beta plays a role in the vasculitis, not in the pathogenesis, of the respiratory epithelium.

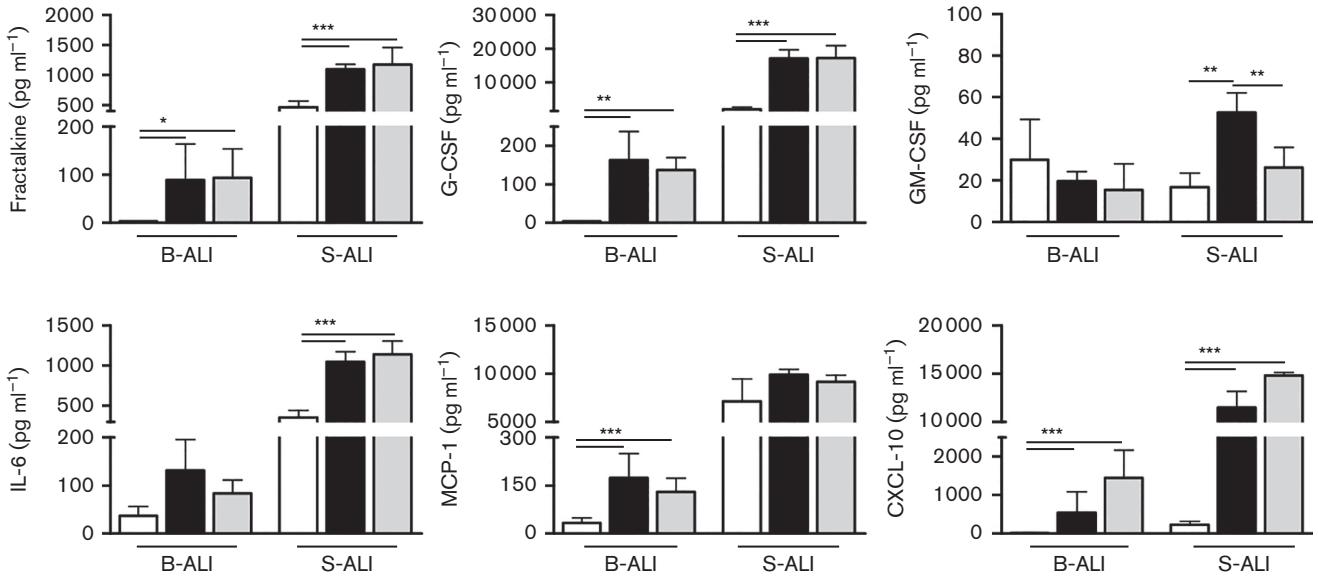

Fig. 5. Quantification of cytokines and chemokines secreted by B- and S-ALI. Cytokines/chemokines secreted from the basal side of control (white) or high m.o.i. NiV-M-infected (black) and NiV-B-infected (grey) B- and S-ALI at day 7 p.i. Results are expressed as the mean of three biological repetitions and bars represent standard deviation. *$P<0.05$, **$P<0.01$ and ***$P<0.001$, ANOVA, Bonferroni's multiple comparison test.

In conclusion, our results show that the tracheal/bronchial and small airway epithelial models are novel biologically relevant systems to study NiV pathogenesis of the human lower respiratory tract epithelium. Both NiV-M and NiV-B infected the same cell types in B- and S-ALI, and induced similar inflammatory responses that seem to be specific to each of the tracheal/bronchial and small airway epithelium. The inflammatory response of NiV-infected S-ALI, but not B-ALI, resulted in recruitment of immune cells regardless of the virus strain used. Finally, a high level of NiV replication in B-ALI, in the absence of inflammatory cell migration, suggests that the human tracheal/bronchial epithelium is an opportune location for early replication, aerosolization and shedding of infectious virus particles. This is consistent with the fact that human-to-human transmission was reported during the outbreak in 2004 in Bangladesh where direct exposure to respiratory secretions of infected patients was associated with infection (Gurley *et al.*, 2007). *In vitro* models mimicking the normal human pulmonary physiology such as B- and S-ALI are essential for understanding the early host–pathogen interactions and mechanisms of henipavirus pathogenesis to identify molecular targets and develop therapeutics as well as to provide fundamental insights into human-to-human transmission potential.

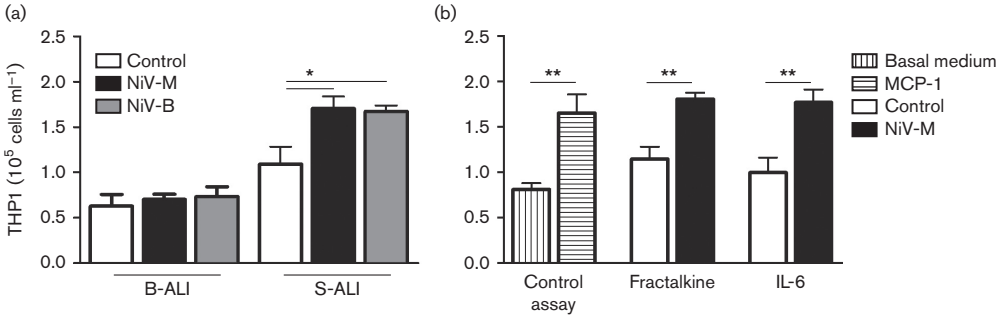

Fig. 6. Monocyte chemotaxis in NiV-M- and NiV-B-infected B- and S-ALI. Monocyte chemotaxis assay was performed using mixtures similar to the basal side of B- and S-ALI cultures (a), or samples made of only one cytokine or chemokine at a time (b), as described in Methods. Quantification of monocytes per sample is expressed as the mean of three technical repetitions and bars represent standard deviation. *$P<0.05$, **$P<0.01$, non-parametric Mann–Whitney test.

METHODS

Viruses and cells. NiV-Malaysia (NiV-M) and NiV-Bangladesh (NiV-B) viruses were provided by the Special Pathogens Branch (Centers for Disease Control and Prevention, GA, USA). NiV-M was originally isolated from the cerebrospinal fluid (CSF) of a patient with encephalitis during the outbreak in Malaysia and Singapore in 1998. NiV-B was isolated from a throat swab of a patient exhibiting respiratory involvement during the 2004 outbreak in Rajbari district, Bangladesh. The viruses were propagated and titrated on Vero cells (CCL-81; ATCC) as previously described (Escaffre *et al.*, 2013). Normal human bronchial epithelial cells were delivered ready to use after 2 weeks of differentiation on inserts with an air–liquid interface (ALI) (MatTek Corporation), providing the B-ALI model. Normal human small airway epithelial cells derived from the distal airspace were also cultured in flasks and differentiated for 2 weeks on inserts with an ALI procedure following the manufacturer's instructions (Clonetics), providing the S-ALI model. All cells originated from biopsies in two healthy donors. Both models were checked, after 2 weeks of ALI procedure, for cilia expression and beating, and for surfactant secretion before infection, using an upright microscope at $\times 40$ magnification. B- and S-ALI were also checked for barrier formation by measuring transepithelial electric resistance using the EVOM2 epithelial voltohmmeter (World Precision Instruments). Prior to virus inoculation, the apical side of inserts was washed with 250 µl of 1 × PBS and infected with 150 µl virus at an m.o.i. of 0.1 or 1 (virus replication kinetics), or 1 (cellular tropism, cytokine/chemokine quantification and chemotaxis assay). The m.o.i. was calculated based on the number of cells originally used to seed the inserts. Following a 1 h incubation at 37 °C, the apical side of inserts was rinsed three times with 200 µl of 1 × PBS, and all liquid was removed from the surface in order to maintain the differentiation process. Each condition was performed with biological triplicates. Sampling for virus replication kinetics was performed from the apical side by washing the cells with 200 µl of 1 × PBS. Cytokines/chemokines quantification was performed using samples from the basolateral side. All infectious work was performed in a class II biological safety cabinet in a biosafety level 4 laboratory (BSL4) at the Galveston National Laboratory, University of Texas Medical Branch.

Bright-field and fluorescence microscopy. Cells on inserts were fixed using 4 % paraformaldehyde (PFA) for 48 h, and then for 24 h with fresh 4 % PFA before transfer to the BSL2 for paraffin embedding and sectioning. Sections were then processed and imaged with an Evos XL core when haematoxylin and eosin staining was used, and with an Olympus IS71 microscope for fluorescence detection. Primary antibodies against ciliated cells (mouse anti-alpha-tubulin; Invitrogen), goblet cells (rabbit anti-Muc5AC; Abcam) and Clara cells (mouse anti-CC10 antibody; Santa Cruz) were detected using a secondary rhodamine red goat anti-mouse antibody (Jackson ImmunoResearch), an AF488 goat anti-rabbit antibody or an AF594 goat anti-rabbit antibody (Life Technologies). Viral antigen was detected using a rabbit anti-NiV-nucleoprotein antibody (kindly provided by Dr C. Broder, Uniformed Services University, Bethesda, Maryland) and an AF488 goat anti-rabbit antibody (Life Technologies) as secondary antibody. DAPI staining (Sigma) was added to visualize cell nuclei.

Scanning electron microscopy. Cells on inserts were fixed for 48 h in a mixture of 2.5 % formaldehyde and 0.1 % glutaraldehyde in 0.05 M cacodylate buffer (pH 7.2) containing 0.01 % trinitrophenol and 0.03 % $CaCl_2$ (primary fixative) and then with fresh primary fixative for 24 h prior to removal from BSL4. Fixed samples were washed in 0.1 M cacodylate buffer, post-fixed in 1 % OsO_4 in 0.1 M cacodylate buffer (pH 7.3), dehydrated in ethanol and processed through hexamethyldisilazane. After being air-dried, filters were detached, mounted onto the specimen stubs and sputter-coated with iridium in an Emitech K575x sputter coater at 20 mA for 20 s. Samples were examined in a Hitachi S4700 field emission scanning electron microscope (Hitachi High Technologies America) at 2 kV and instrumental magnifications from $\times 35$ to $\times 50\,000$.

Cytokine/chemokine analysis. Cytokine/chemokine concentrations in the supernatant of NiV-M- and NiV-B-infected B- and S-ALI were determined using a Milliplex Human Cytokine 15 Plex Immunoassay custom kit (Millipore) and a Verikine-HS Human IFN Beta ELISA kit (PBL Assay Science). Prior to analysis, samples were inactivated on dry ice by gamma irradiation (5 Mrad). The assays were performed according to the manufacturer's instructions. The concentration of 16 cytokines [granulocyte-colony stimulating factor (G-CSF), granulocyte macrophage-colony stimulating factor (GM-CSF), IFN-α2, IFNβ, IFNγ, IL-1α, IL-1β, IL-6, IL-8, IL-1RA, chemokine ligand 10 (CXCL10), eotaxin, monocyte chemotactic protein (MCP-1), TNF-α, fractalkine (CX3CL1) and vascular endothelial growth factor A (VEGF)] were quantified.

Chemotaxis assay. For analysing immune cell migration, 1.6×10^6 THP-1 monocytes per sample were washed twice with serum-free RPMI 1640, warmed to 37 °C, and plated in the top chamber of an 8 µm transwell in 200 µl of serum-free RPMI 1640. Each transwell insert was then placed into a bottom chamber containing 500 µl of either serum-free RPMI 1640 (negative control), serum-free RPMI 1640 with mixtures of recombinant human cytokines and chemokines, serum-free RPMI 1640 with one cytokine or chemokine, or serum-free RPMI 1640 with 50 ng MCP-1 ml^{-1} (positive control). The cytokines and chemokines (Shenandoah Biotechnology) were used at concentrations similar to those observed in the basolateral medium of B- and S-ALI cultures, at day 7 p.i., based on the Milliplex data. Cytokines and chemokines tested included G-CSF, GM-CSF, fractalkine, IL-6, MCP-1 and CXCL10 that were tested as a pool or individually for monocyte chemotactic activity. Monocytes were allowed to migrate for 3 h at 37 °C in the bottom chamber, and were then counted using an automated cell counter (Millipore).

Statistical analyses. Comparisons of virus replication levels and number of migrated monocytes due to chemotaxis were performed using the non-parametric Mann–Whitney test. Comparison of cytokine/chemokine secretion levels was subjected to a repeated measure one-way ANOVA test followed by a Bonferroni's multiple comparison test to determine whether treatment means were significantly different from one another. All data are presented in figures as means ± SD ($*P<0.05$, $**P<0.01$, $***P<0.001$). Each condition was performed with biological triplicates.

ACKNOWLEDGEMENTS

This work was supported by the University of Texas Medical Branch (UTMB) startup funds and National Institutes of Health [1R21AI111042-01] to B. R., and an UTMB Center for Tropical Diseases Postdoctoral Fellowship to O. E. The authors would like to thank Dr Alexander N. Freiberg for helpful discussions and Dr Vsevolod Popov for technical assistance in specimen preparation and electron microscopy.

REFERENCES

Baggiolini, M., Imboden, P. & Detmers, P. (1992). Neutrophil activation and the effects of interleukin-8/neutrophil-activating peptide 1 (IL-8/NAP-1). *Cytokines* **4**, 1–17.

Baseler, L., de Wit, E., Scott, D. P., Munster, V. J. & Feldmann, H. (2015). Syrian hamsters (*Mesocricetus auratus*) oronasally inoculated

with a Nipah virus isolate from Bangladesh or Malaysia develop similar respiratory tract lesions. *Vet Pathol* **52**, 38–45.

Bossart, K. N., Rockx, B., Feldmann, F., Brining, D., Scott, D., LaCasse, R., Geisbert, J. B., Feng, Y. R., Chan, Y. P. & other authors (2012). A Hendra virus G glycoprotein subunit vaccine protects African green monkeys from Nipah virus challenge. *Sci Transl Med* **4**, 146ra107.

Chong, H. T., Kunjapan, S. R., Thayaparan, T., Tong, J. M. G., Petharunam, V., Jusoh, M. R. & Tan, C. T. (2002). Nipah encephalitis outbreak in Malaysia, clinical features in patients from Seremban. *Can J Neurol Sci* **29**, 83–87.

Chua, K. B., Bellini, W. J., Rota, P. A., Harcourt, B. H., Tamin, A., Lam, S. K., Ksiazek, T. G., Rollin, P. E., Zaki, S. R. & other authors (2000). Nipah virus: a recently emergent deadly paramyxovirus. *Science* **288**, 1432–1435.

Chua, K. B., Lam, S. K., Goh, K. J., Hooi, P. S., Ksiazek, T. G., Kamarulzaman, A., Olson, J. & Tan, C. T. (2001). The presence of Nipah virus in respiratory secretions and urine of patients during an outbreak of Nipah virus encephalitis in Malaysia. *J Infect* **42**, 40–43.

Clahsen, T. & Schaper, F. (2008). Interleukin-6 acts in the fashion of a classical chemokine on monocytic cells by inducing integrin activation, cell adhesion, actin polymerization, chemotaxis, and transmigration. *J Leukoc Biol* **84**, 1521–1529.

de Wit, E., Prescott, J., Falzarano, D., Bushmaker, T., Scott, D., Feldmann, H. & Munster, V. J. (2014). Foodborne transmission of nipah virus in Syrian hamsters. *PLoS Pathog* **10**, e1004001.

DeBuysscher, B. L., de Wit, E., Munster, V. J., Scott, D., Feldmann, H. & Prescott, J. (2013). Comparison of the pathogenicity of Nipah virus isolates from Bangladesh and Malaysia in the Syrian hamster. *PLoS Negl Trop Dis* **7**, e2024.

Eaton, B. T., Broder, C. C. & Wang, L. F. (2005). Hendra and Nipah viruses: pathogenesis and therapeutics. *Curr Mol Med* **5**, 805–816.

Escaffre, O., Borisevich, V., Carmical, J. R., Prusak, D., Prescott, J., Feldmann, H. & Rockx, B. (2013). Henipavirus pathogenesis in human respiratory epithelial cells. *J Virol* **87**, 3284–3294.

Gerlach, R. L., Camp, J. V., Chu, Y. K. & Jonsson, C. B. (2013). Early host responses of seasonal and pandemic influenza A viruses in primary well-differentiated human lung epithelial cells. *PLoS One* **8**, e78912.

Goh, K. J., Tan, C. T., Chew, N. K., Tan, P. S., Kamarulzaman, A., Sarji, S. A., Wong, K. T., Abdullah, B. J., Chua, K. B. & Lam, S. K. (2000). Clinical features of Nipah virus encephalitis among pig farmers in Malaysia. *N Engl J Med* **342**, 1229–1235.

Gurley, E. S., Montgomery, J. M., Hossain, M. J., Bell, M., Azad, A. K., Islam, M. R., Molla, M. A., Carroll, D. S., Ksiazek, T. G. & other authors (2007). Person-to-person transmission of Nipah virus in a Bangladeshi community. *Emerg Infect Dis* **13**, 1031–1037.

Harit, A. K., Ichhpujani, R. L., Gupta, S., Gill, K. S., Lal, S., Ganguly, N. K. & Agarwal, S. P. (2006). Nipah/Hendra virus outbreak in Siliguri, West Bengal, India in 2001. *J Med Res* **123**, 553–560.

Hooper, P., Zaki, S., Daniels, P. & Middleton, D. (2001). Comparative pathology of the diseases caused by Hendra and Nipah viruses. *Microbes Infect* **3**, 315–322.

Hossain, M. J., Gurley, E. S., Montgomery, J. M., Bell, M., Carroll, D. S., Hsu, V. P., Formenty, P., Croisier, A., Bertherat, E. & other authors (2008). Clinical presentation of nipah virus infection in Bangladesh. *Clin Infect Dis* **46**, 977–984.

Imai, T., Hieshima, K., Haskell, C., Baba, M., Nagira, M., Nishimura, M., Kakizaki, M., Takagi, S., Nomiyama, H. & other authors (1997). Identification and molecular characterization of fractalkine receptor CX3CR1, which mediates both leukocyte migration and adhesion. *Cell* **91**, 521–530.

Lam, E., Ramke, M., Warnecke, G., Schrepfer, S., Kopfnagel, V., Dobner, T. & Heim, A. (2015). Effective apical infection of differentiated human bronchial epithelial cells and induction of proinflammatory chemokines by the highly pneumotropic human adenovirus type 14p1. *PLoS One* **10**, e0131201.

Levitzky, M. G. (2013). *Pulmonary Physiology*, 8th edn. New York: McGraw-Hill.

Lo, M. K. & Rota, P. A. (2008). The emergence of Nipah virus, a highly pathogenic paramyxovirus. *J Clin Virol* **43**, 396–400.

Lo, M. K., Miller, D., Aljofan, M., Mungall, B. A., Rollin, P. E., Bellini, W. J. & Rota, P. A. (2010). Characterization of the antiviral and inflammatory responses against Nipah virus in endothelial cells and neurons. *Virology* **404**, 78–88.

Luster, A. D. & Leder, P. (1993). IP-10, a -C-X-C- chemokine, elicits a potent thymus-dependent antitumor response in vivo. *J Exp Med* **178**, 1057–1065.

Matrosovich, M. N., Matrosovich, T. Y., Gray, T., Roberts, N. A. & Klenk, H. D. (2004). Human and avian influenza viruses target different cell types in cultures of human airway epithelium. *Proc Natl Acad Sci U S A* **101**, 4620–4624.

Mercer, R. R., Russell, M. L., Roggli, V. L. & Crapo, J. D. (1994). Cell number and distribution in human and rat airways. *Am J Respir Cell Mol Biol* **10**, 613–624.

Mitchell, H., Levin, D., Forrest, S., Beauchemin, C. A., Tipper, J., Knight, J., Donart, N., Layton, R. C., Pyles, J. & other authors (2011). Higher level of replication efficiency of 2009 (H1N1) pandemic influenza virus than those of seasonal and avian strains: kinetics from epithelial cell culture and computational modeling. *J Virol* **85**, 1125–1135.

Mounts, A. W., Kaur, H., Parashar, U. D., Ksiazek, T. G., Cannon, D., Arokiasamy, J. T., Anderson, L. J., Lye, M. S. & Nipah Virus Nosocomial Study Group (2001). A cohort study of health care workers to assess nosocomial transmissibility of Nipah virus, Malaysia, 1999. *J Infect Dis* **183**, 810–813.

Paton, N. I., Leo, Y. S., Zaki, S. R., Auchus, A. P., Lee, K. E., Ling, A. E., Chew, S. K., Ang, B., Rollin, P. E. & other authors (1999). Outbreak of Nipah-virus infection among abattoir workers in Singapore. *Lancet* **354**, 1253–1256.

Ren, D., Nelson, K. L., Uchakin, P. N., Smith, A. L., Gu, X. X. & Daines, D. A. (2012). Characterization of extended co-culture of non-typeable *Haemophilus influenzae* with primary human respiratory tissues. *Exp Biol Med (Maywood)* **237**, 540–547.

Rock, J. R., Randell, S. H. & Hogan, B. L. (2010). Airway basal stem cells: a perspective on their roles in epithelial homeostasis and remodeling. *Dis Model Mech* **3**, 545–556.

Rockx, B., Sheahan, T., Donaldson, E., Harkema, J., Sims, A., Heise, M., Pickles, R., Cameron, M., Kelvin, D. & Baric, R. (2007). Synthetic reconstruction of zoonotic and early human severe acute respiratory syndrome coronavirus isolates that produce fatal disease in aged mice. *J Virol* **81**, 7410–7423.

Rockx, B., Brining, D., Kramer, J., Callison, J., Ebihara, H., Mansfield, K. & Feldmann, H. (2011). Clinical outcome of henipavirus infection in hamsters is determined by the route and dose of infection. *J Virol* **85**, 7658–7671.

Rockx, B., Winegar, R. & Freiberg, A. N. (2012). Recent progress in henipavirus research: molecular biology, genetic diversity, animal models. *Antiviral Res* **95**, 135–149.

Tan, C. T. & Tan, K. S. (2001). Nosocomial transmissibility of Nipah virus. *J Infect Dis* **184**, 1367.

Taub, D. D., Lloyd, A. R., Conlon, K., Wang, J. M., Ortaldo, J. R., Harada, A., Matsushima, K., Kelvin, D. J. & Oppenheim, J. J. (1993). Recombinant human interferon-inducible protein 10 is a

chemoattractant for human monocytes and T lymphocytes and promotes T cell adhesion to endothelial cells. *J Exp Med* **177**, 1809–1814.

Thelen, M. (2001). Dancing to the tune of chemokines. *Nat Immunol* **2**, 129–134.

Valbuena, G., Halliday, H., Borisevich, V., Goez, Y. & Rockx, B. (2014). A human lung xenograft mouse model of Nipah virus infection. *PLoS Pathog* **10**, e1004063.

Weissenbach, M., Clahsen, T., Weber, C., Spitzer, D., Wirth, D., Vestweber, D., Heinrich, P. C. & Schaper, F. (2004). Interleukin-6 is a direct mediator of T cell migration. *Eur J Immunol* **34**, 2895–2906.

Wong, K. T., Shieh, W. J., Kumar, S., Norain, K., Abdullah, W., Guarner, J., Goldsmith, C. S., Chua, K. B., Lam, S. K. & other authors (2002). Nipah virus infection: pathology and pathogenesis of an emerging paramyxoviral zoonosis. *Am J Pathol* **161**, 2153–2167.